Int. J. Heat Mass Transfer. Vol. 33, No. 9, pp. 1977–1986, 1990
Printed in Great Britain

0017-9310/90 $3.00 + 0.00

Codeposition of SiO_2/GeO_2 during production of optical fiber preforms by modified chemical vapor deposition

KYO-SEON KIM† and SOTIRIS E. PRATSINIS‡

Department of Chemical Engineering, Center for Aerosol Processes, University of Cincinnati, Cincinnati, OH 45221-0171, U.S.A.

(*Received* 18 *January* 1989 *and in final form* 27 *November* 1989)

Abstract—A theoretical study of simultaneous chemistry, heat and mass transfer during the so-called multicomponent modified chemical vapor deposition (MCVD) process for fabrication of lightguide preforms is presented. Codeposition of SiO_2 and GeO_2 is examined since these are the dominant species of lightguides for telecommunications. The full Navier–Stokes equations for this process are solved, including continuity, momentum, energy and mass balances for gases and SiO_2 and GeO_2 particles. The $GeCl_4$ conversion and deposition efficiency decrease as inlet $SiCl_4$ concentration increases. At high overall gas flow rates through the preform tube and low inlet $SiCl_4$ concentrations, the $GeCl_4$ yield is limited by $GeCl_4$ conversion while at low gas flow rates or high inlet $SiCl_4$ concentrations, the $GeCl_4$ yield is limited by particle transport.

INTRODUCTION

TODAY, optical fibers are no longer just high technology materials but have become commodity products, so even marginal increases in process yields can have a substantial economic impact. The manufacture of optical fibers also involves a unique combination of chemistry, aerosol dynamics and transport phenomena. Thus, quantitative understanding of optical fiber preform fabrication processes is a topic of both scientific and engineering interest.

More than half of the worldwide production of optical waveguide preforms is made by the so-called modified chemical vapor deposition (MCVD) process. In this process, halide ($SiCl_4$, $GeCl_4$, $POCl_3$, BCl_3) vapors are supplied with O_2 to a rotating fused silica tube which is externally heated by a slowly, axially traversing, oxy-hydrogen torch. There, the halides are oxidized at high temperature forming oxide particles which either deposit to the tube walls or exit the tube with the process gases. The fabrication of the preform rod is completed when the successively deposited particle layers (30–100) almost fill the substrate tube [1].

Germania is the most common dopant for raising the refractive index of graded index optical fiber. In MCVD, the incorporation of GeO_2 is low due to unfavorable equilibrium of the $GeCl_4$ oxidation reaction at high temperature in the presence of $SiCl_4$ [2].

After the MCVD process was invented for fabrication of optical fiber preforms [3], thermophoresis was proven to be the dominant mass transfer mechanism experimentally [4] and theoretically [5]. Morse *et al.* [6–8] showed that the deposition efficiency can be enhanced by using axial laser heating in MCVD preform tubes. Fiebig *et al.* [9] proposed that the deposition efficiency and rate in MCVD can be increased by inserting and maintaining at high temperature a concentric annular tube inside the preform. Wood *et al.* [2] experimentally investigated the incorporation of germania in MCVD of lightguide preforms by varying the torch temperature, reactant composition and gas flow rates and proposed a simple model predicting the extent of germania incorporation in the preform deposit. Kim and Pratsinis [10–12] first developed a model of the MCVD process accounting for simultaneous gas phase chemistry, heat and mass transfer and silica oxide aerosol dynamics during MCVD of lightguide preforms. It was shown that rapid coagulation of the newly formed silica particles in the preform reaction zone makes thermophoresis the dominant mass transfer mechanism in the deposition zone of the preform. The evolution of the silica aerosol along the preform axis was described and it was found that radial diffusion of $SiCl_4$ in the preform reaction zone results in high SiO_2 concentrations in the vicinity of the preform inner tube wall. The effect of different carrier gases on SiO_2 deposition rate and efficiency was also investigated and the MCVD deposition efficiency was mapped in the parameter space of process gas flow and inlet $SiCl_4$ concentration.

In this paper, we extend our earlier work [12] to the description of multicomponent (SiO_2 and GeO_2) MCVD. In the present analysis, the reversibility of the $GeCl_4$ reaction is accounted for as well as the

† Present address: Department of Chemical Engineering, Kangwon National University, Seoul, Korea.
‡ Author to whom all correspondence should be addressed.

NOMENCLATURE

a	activity in GeO_2/SiO_2 particles, γY
C	gas concentration [mol cm^{-3}]
C_p	heat capacity of gas [J mol^{-1} K^{-1}]
C_{p0}, C_{p1}, C_{p2}	constants for calculation of heat capacity
D	diffusivity in carrier gas [cm^2 s^{-1}]
$D_{CL,0}$, $D_{GC,0}$, $D_{O2,0}$, $D_{SC,0}$	constants to calculate diffusivities of Cl_2, $GeCl_4$, O_2 and $SiCl_4$ in carrier gas
E_{GC}	activation energy for oxidation of $GeCl_4$ [J mol^{-1}]
E_{SC}	activation energy for oxidation of $SiCl_4$ [J mol^{-1}]
E_D	deposition efficiency
E_R	conversion
ΔH	heat of reaction [J mol^{-1}]
k	heat conductivity of carrier gas [cal cm^{-1} K^{-1} s^{-1}]
$k_{GC,0}$	frequency factor for $GeCl_4$ oxidation [s^{-1}]
k_{GC}	rate constants for $GeCl_4$ oxidation
$k_{SC,0}$, $k_{SC,1}$	constants for $SiCl_4$ oxidation rate
k_0, k_1, k_2	constants to calculate heat conductivity of gas
K	thermophoretic coefficient
K_{EQ}	equilibrium constant of $GeCl_4$ oxidation
$K_{EQ,C}$	constant of $GeCl_4$ oxidation, $Y_{GO}X_{CL}^2/X_{GC}X_{O2}$
L_1, L_2	axial distances in the reaction zone
M	molecular weight of gas mixture
n_i	moles of i species particles per mole of carrier gas, N_i/C
N_i	moles of i species particles per unit volume
p	pressure
P	number of radial points for finite-difference method
Q	total gas flow rate through the preform tube at 298 K [1 min^{-1}]
r	radial distance [cm]
r_{GC}	rate of formation of GeO_2 particles by oxidation [cm^{-3} s^{-1}]
r_{SC}	rate of formation of SiO_2 particles by oxidation [cm^{-3} s^{-1}]
R	reactor radius [cm]
R_G	gas constant, 82.06 cm^3 atm mol^{-1} K^{-1}
T	gas temperature [K]
T_{max}	maximum tube temperature (just above oxy-hydrogen torch) [K]
T_{min}	minimum tube temperature (downstream of the torch) [K]
u	axial velocity [cm s^{-1}]
U	average gas velocity at the inlet [cm s^{-1}]
v	radial velocity [cm s^{-1}]
V_P	net particle velocity in the radial direction, $v+V_T$ [cm s^{-1}]
V_T	thermophoretic velocity of particles in the radial direction [cm s^{-1}]
X	mole fraction in the gas phase
Y_i	mole fraction in the particle phase, $n_i/(n_{GO}+n_{SO})$
z	axial distance of reactor [cm].

Greek symbols

α	thermal diffusivity of carrier gas, $k/\rho C_p$ [cm^2 s^{-1}]
γ	activity coefficient of GeO_2 in GeO_2/SiO_2 particle phase
μ	viscosity of gas stream [g cm^{-1} s^{-1}]
ν	kinematic viscosity [cm^2 s^{-1}]
ν_0	constant for calculation of kinematic viscosity
ρ	density of gas stream [g cm^{-3}].

Subscripts

CL	Cl_2
GC	$GeCl_4$
GO	GeO_2
m	mixing cup average
O2	O_2
SC	$SiCl_4$
SO	SiO_2
w	wall
z	at axial distance z
0	inlet condition
+1	for forward reaction
−1	for backward reaction.

simultaneous reaction kinetics and transport phenomena of $SiCl_4$ and $GeCl_4$ in MCVD of lightguide preforms. The variation of the $GeCl_4$ yield (one of the most costly dopants in MCVD [13]) is examined at various process parameters such as overall gas flow rate, maximum torch temperature and inlet $SiCl_4$ concentration.

THEORY

In the MCVD process, a mixture of reactants ($SiCl_4$, $GeCl_4$ and O_2) is fed into a silica tube (reactor) in fully developed laminar flow. There, the mixture is heated by an external heat source (reaction zone) and exothermic oxidation of $SiCl_4$ and $GeCl_4$ takes place forming SiO_2, GeO_2 and Cl_2. The temperature inside the tube increases further by the released heat of reactions. As the gas stream leaves the reaction zone, it flows into the deposition zone where it cools down by heat transfer to the low-temperature tube wall. There, fractions of newly formed silica and germania particles are deposited to the tube wall mostly by thermophoresis, while the rest exit the preform tube by convection.

Each mole of $SiCl_4$ and $GeCl_4$ requires one mole of

O_2 to form two moles of Cl_2 in the gas phase and the total number of moles in the gas phase is conserved throughout the MCVD process. Thus, the continuity equation can be written in terms of molar density as

$$\frac{\partial}{\partial z}(Cu)+\frac{1}{r}\frac{\partial}{\partial r}(Crv)=0. \quad (1)$$

Following the analysis of Walker *et al.* (Appendix A of ref. [5]), the momentum balance in the z-direction is

$$Cu\frac{\partial u}{\partial z}+Cv\frac{\partial u}{\partial r}=-\frac{1}{M}\frac{dp}{dz}+\frac{1}{Mr}\frac{\partial}{\partial r}\left(\mu r\frac{\partial u}{\partial r}\right). \quad (2)$$

The terms on the left-hand side (LHS) show the change of convective z-momentum flow and the first term on the right-hand side (RHS) accounts for the pressure force along the preform axis while the second RHS term accounts for the viscous dissipation rate. The process conditions employed during MCVD allow the neglect of natural convection [8, 14]. Also, the rotation of the fused silica tube with frequency of about 1 Hz suppresses the natural convection inside the tube [9]. The radial momentum balance equation degenerates to render $\partial p/\partial r = 0$ in reduced form and p becomes a function of z only [5].

Extending the analysis of Walker *et al.* [5] in reactive flows and neglecting the effect of particles on gas properties and the axial heat diffusion compared to forced convection, the energy balance equation for MCVD is

$$Cu\frac{\partial}{\partial z}(C_pT)+Cv\frac{\partial}{\partial r}(C_pT)=\frac{1}{r}\frac{\partial}{\partial r}\left(kr\frac{\partial T}{\partial r}\right)+\Delta H_{SC}r_{SC}+\Delta H_{GC}r_{GC}. \quad (3)$$

The LHS terms in equation (3) describe the heat transfer by convection. The first RHS term accounts for the radial heat transfer by conduction and the remaining terms for heat generation by oxidation of $SiCl_4$ and $GeCl_4$. The heats of reaction are calculated for the reaction products of solid silica and liquid germania. The $SiCl_4$ oxidation rate is [15]

$$r_{SC}=(k_{SC,0}+k_{SC,1}CX_{O2})\exp(-E_{SC}/R_GT)CX_{SC}. \quad (4)$$

The oxidation of $GeCl_4$ is reversible [2]

$$r_{GC}=k_{GC,+1}C_{GC}C_{O2}-k_{GC,-1}a_{GO}C_{CL}^2 \quad (5)$$

$$=k_{GC,0}\exp(-E_{GC}/R_GT)C^2(X_{GC}X_{O2}-\gamma Y_{GO}X_{CL}^2/K_{EQ}). \quad (6)$$

French *et al.* [16] measured the oxidation rate of $GeCl_4$ in an O_2 rich environment and presented the value of $k_{GC,0}C_{O2}$ ($=0.20\times10^{10}$ s^{-1}) assuming first-order, irreversible reaction with respect to $GeCl_4$. By calculating the C_{O2} at 1400 K [16], the $k_{GC,0}$ is 2.3×10^{15} cm^3 mol^{-1} s^{-1}. The K_{EQ} is obtained in general form by interpolating the data of Wood *et al.* [2] in the temperature range, 300–1800 K

$$\ln K_{EQ}=-98.33-2.2525\times10^{-3}T+19\,690/T+12.01\ln T. \quad (7)$$

It should be noted that the particle phase is assumed to be an ideal solution ($\gamma = 1$) and that the particle surface reaction is assumed to be negligible. The dissociation of Cl_2 into Cl and the volatilization of GeO_2 into GeO affect the germania incorporation in optical preform fabrication only slightly [2] and both reactions are neglected in the present analysis.

Assuming negligible axial mass diffusion compared to convection and negligible Soret diffusion of gas species, the mass balance equations for $SiCl_4$, $GeCl_4$, O_2 and Cl_2 are

$$Cu\frac{\partial}{\partial z}X_{SC}+Cv\frac{\partial}{\partial r}X_{SC}=\frac{1}{r}\frac{\partial}{\partial r}\left(CD_{SC}r\frac{\partial}{\partial r}X_{SC}\right)-r_{SC} \quad (8)$$

$$Cu\frac{\partial}{\partial z}X_{GC}+Cv\frac{\partial}{\partial r}X_{GC}=\frac{1}{r}\frac{\partial}{\partial r}\left(CD_{GC}r\frac{\partial}{\partial r}X_{GC}\right)-r_{GC} \quad (9)$$

$$Cu\frac{\partial}{\partial z}X_{O2}+Cv\frac{\partial}{\partial r}X_{O2}=\frac{1}{r}\frac{\partial}{\partial r}\left(CD_{O2}r\frac{\partial}{\partial r}X_{O2}\right)-r_{SC}-r_{GC} \quad (10)$$

$$Cu\frac{\partial}{\partial z}X_{CL}+Cv\frac{\partial}{\partial r}X_{CL}=\frac{1}{r}\frac{\partial}{\partial r}\left(CD_{CL}r\frac{\partial}{\partial r}X_{CL}\right)+2r_{SC}+2r_{GC} \quad (11)$$

The LHS terms in equations (8)–(11) are the mass transfer rates by convection, the first RHS terms account for the diffusion of gas components in the radial direction and the remaining RHS terms account for the mass losses or gains by chemical reactions.

Neglecting silica and germania particle diffusion in both radial and axial directions, the mass balance equations for SiO_2 and GeO_2 are written as

$$Cu\frac{\partial}{\partial z}n_{SO}+Cv\frac{\partial}{\partial r}n_{SO}=\frac{1}{r}\frac{\partial}{\partial r}\left(CKvn_{SO}r\frac{\partial}{\partial r}\ln T\right)+r_{SC} \quad (12)$$

$$Cu\frac{\partial}{\partial z}n_{GO}+Cv\frac{\partial}{\partial r}n_{GO}=\frac{1}{r}\frac{\partial}{\partial r}\left(CKvn_{GO}r\frac{\partial}{\partial r}\ln T\right)+r_{GC} \quad (13)$$

where n_{SO} and n_{GO} are the number of SiO_2 and GeO_2 moles per mole of gas, respectively. The LHS terms in equations (12) and (13) are the particle transfer rates by convection, and the first RHS terms account for thermophoresis of particles in the radial direction; the second RHS terms are the generation rates of SiO_2 and GeO_2 by chemical reactions. The thermophoretic

coefficient, K, is constant and equal to 0.55 for the particles of SiO_2 and GeO_2 less than 0.2 μm in diameter at the operating temperature of the MCVD process [11].

Assuming that the inlet temperature and reactant concentrations are uniform for all r, the gas mixture enters the tube with a parabolic velocity profile and is free of silica and germania particles and chlorine, the initial conditions are given at $z = 0$ for all r as

$$T = T_0, \quad u = 2U(1-(r/R)^2), \quad v = 0, \quad p = p_0,$$
$$X_{SC} = X_{SC,0}, \quad X_{GC} = X_{GC,0}, \quad X_{O2} = X_{O2,0},$$
$$X_{CL} = 0, \quad n_{SO} = N_{GO} = 0. \tag{14}$$

By cylindrical symmetry, the boundary conditions at $r = 0$ for all z are

$$\frac{\partial T}{\partial r} = \frac{\partial u}{\partial r} = \frac{\partial}{\partial r}X_{SC} = \frac{\partial}{\partial r}X_{GC} = \frac{\partial}{\partial r}X_{O2} = \frac{\partial}{\partial r}X_{CL} = \frac{\partial}{\partial r}n_{SO} = \frac{\partial}{\partial r}n_{GO} = v = 0. \tag{15}$$

The tube wall temperature profile in the MCVD process is given as a function of axial distance [7]. Assuming that all particles arriving at the tube wall stick there and the chemical vapor deposition rates of $SiCl_4$ and $GeCl_4$ at the tube wall are negligible compared to the $SiCl_4$ and $GeCl_4$ oxidation rates in the gas phase, the boundary conditions at the tube wall ($r = R$) in the reaction zone are

$$T_w(z) = T_0 + (T_{max} - T_0)(z/L_1)^2 \quad \text{for } 0 \leqslant z \leqslant L_1 \tag{16a}$$

$$T_w(z) = T_{max} - (T_{max} - T_{min})(z - L_1)/(L_2 - L_1) \quad \text{for } L_1 \leqslant z < L_2 \tag{16b}$$

and in the deposition zone are

$$T_w(z) = T_{min} \quad \text{for } z \geqslant L_2 \tag{16c}$$

$$u = v = n_{SO} = n_{GO} = 0 \quad \text{for all } z \tag{16d}$$

$$\frac{\partial}{\partial r}X_{SC} = \frac{\partial}{\partial r}X_{GC} = \frac{\partial}{\partial r}X_{O2} = \frac{\partial}{\partial r}X_{CL} = 0 \quad \text{for all } z. \tag{16e}$$

The gas properties are given as a function of T and p using literature expressions for viscosity and diffusion [19], heat capacity [20] and thermal conductivity [21] and the gas properties are calculated for the carrier gas of O_2

$$C = p/R_G T \tag{17a}$$

$$\mu/MC = \nu = \nu_0 T^{1.65} \tag{17b}$$

$$C_p = C_{p0} + C_{p1}T - C_{p2}/T^2 \tag{17c}$$

$$k = k_0 + k_1 T + k_2 T^2 \tag{17d}$$

$$D_{SC} = D_{SC,0}T^{1.66} \tag{17e}$$

$$D_{GC} = D_{GC,0}T^{1.66} \tag{17f}$$

$$D_{O2} = D_{O2,0}T^{1.66} \tag{17g}$$

$$D_{CL} = D_{CL,0}T^{1.66}. \tag{17h}$$

The effect of particles on gas transport is neglected assuming that relatively dilute suspensions are employed. Recently, Rosner and Park [17] found that the particle deposition rate in the external processes for lightguide preform fabrication can be higher than that predicted by classic thermophoretic calculations because high mass loadings of particles modify the gas stream velocity and temperature. They also extended their analysis for the aerosol mixture of SiO_2 and GeO_2 in the same process [18]. For the process conditions employed in this paper, the particle mass fraction is less than 0.15 and the enhancement of the deposition rate by high mass loading is not significant (see Fig. 6 in ref. [17]).

Both sides of equations (2), (3) and (8)–(13) are divided by Cu and the z-derivatives are kept on the LHS of each equation. All other terms including r-derivatives and reaction rate terms are kept on the RHS of each equation. By applying an explicit finite-difference scheme at P radial points across the tube [22], $8 \times P$ ordinary differential equations (ODEs) with respect to z are obtained. The ODEs are integrated using an efficient algorithm for stiff equations (DGEAR subroutine [23]). All simulations were carried out with 21 radial points ($P = 21$). The integration step size is determined internally by the DGEAR method and, for each integration step, the pressure gradient, dp/dz, is adjusted by trial and error to meet the continuity and axial momentum balance equations. The modified linear interpolation method is applied for the trial-and-error procedures [24]. The boundary condition for v at the tube wall ($v = 0$ at $r = R$) is checked with a value of the pressure gradient and, if the boundary condition is not satisfied, another value of the pressure gradient is tried [25]. For the present work, the pressure gradient is usually obtained within three iterations and the values of u and v are then calculated [26]. The temperature, axial and radial velocities, mole fractions of $SiCl_4$, $GeCl_4$, Cl_2 and O_2, and the amounts of SiO_2 and GeO_2 per mole of gas are calculated along the reactor axis and radius and the process yields of MCVD ($SiCl_4$, $GeCl_4$ conversions and deposition efficiencies) are calculated from mixing cup averages of $SiCl_4$, $GeCl_4$, SiO_2 and GeO_2 concentrations

$$E_{R,SC} = 1 - (CuX_{SC})_{m,z}/(CuX_{SC})_{m,0} \tag{18a}$$

$$E_{D,SO} = E_{R,SC} - (Cun_{SO})_{m,z}/(CuX_{SC})_{m,0} \tag{18b}$$

$$E_{R,GC} = 1 - (CuX_{GC})_{m,z}/(CuX_{GC})_{m,0} \tag{18c}$$

$$E_{D,GO} = E_{R,GC} - (Cun_{GO})_{m,z}/(CuX_{GC})_{m,0}. \tag{18d}$$

The complete computer program is given in a Ph.D. thesis [26].

RESULTS AND DISCUSSION

The accuracy of the numerical scheme is investigated by comparing its results with the limiting solu-

tions of Worsoe-Schmidt and Leppert [27] in the absence of chemical reactions and the two results are in excellent agreement [12, 26].

Process conditions similar to those employed in industrial units are selected (Table 1) for simulations of the manufacture of lightguide preforms in MCVD with $SiCl_4$ and $GeCl_4$ [2, 4, 5]. The evolution of the radial profiles of T, u, v, X_{SC} and n_{SO} is similar to that for pure $SiCl_4$ oxidation since the heat of reaction for $GeCl_4$ oxidation is 1/5 of that for $SiCl_4$ oxidation. The evolution of T, $X_{GC}/X_{GC,0}$, X_{CL}, $n_{GO}/X_{GC,0}$ and Y_{GO} is shown in Figs. 1(a)–(e) along the preform axis for $Q = 1$ l min^{-1} (lpm), $SiCl_4$ flow rate = 0.51 g min^{-1} ($C_{SC,0} = 3 \times 10^{-6}$ mol cm^{-3}) and $GeCl_4$ flow rate = 0.4 g min^{-1} ($C_{SC,0} = 1.9 \times 10^{-6}$ mol cm^{-3}). At first, the pressure drop with these process conditions at distances up to $z = 30$ cm is 2.8×10^{-6} atm. It is in close agreement with the Hagen–Poiseuille equation [28] which predicts the pressure drop of 2.1×10^{-6} atm with average gas properties at 1000 K.

At $z = 14$ in Fig. 1(a), the gas temperature is higher and peaks earlier than when only $SiCl_4$ is present [12], because the $SiCl_4$ oxidation is expedited by the presence of $GeCl_4$ [16]. The $GeCl_4$ reaction takes place first near the tube wall where the gas temperature is higher than at the tube center (Fig. 1(b)). Thus, the dimensionless GeO_2 volume concentration starts to increase in the region near the tube wall (Fig. 1(c)). Chlorine (Cl_2) is generated by the oxidation of both $SiCl_4$ and $GeCl_4$ (Fig. 1(d)). The oxidation of $GeCl_4$ starts earlier ($z = 10$) than $SiCl_4$ ($z = 12$) in the MCVD preform because the activation energy for the former reaction is lower than for the latter. Until $z = 12$ cm, most of Cl_2 comes from the oxidation of $GeCl_4$ and the GeO_2 mole fraction in the particle phase (Y_{GO}) is close to unity since most of the product particles are made of GeO_2 (Fig. 1(e)). The forward reaction of $GeCl_4$ oxidation is dominant until $z = 14$ and the $GeCl_4$ concentration decreases and the GeO_2 volume increases. At $z = 14$, the $SiCl_4$ reaction takes place quickly and the Cl_2 concentration increases and Y_{GO} decreases quickly.

The reaction equilibrium constant for $GeCl_4$ oxidation (K_{EQ}) decreases with temperature according to equation (7) (Fig. 1(f)). The comparison of K_{EQ} and $K_{EQ,C}$ shows how close the $GeCl_4$ reaction is to the equilibrium state. If K_{EQ} is larger than $K_{EQ,C}$, the forward reaction is faster than the backward reaction and $GeCl_4$ conversion increases. For K_{EQ} less than $K_{EQ,C}$, the $GeCl_4$ conversion decreases and, if K_{EQ} and $K_{EQ,C}$ are close, the $GeCl_4$ reaction is in a state of equilibrium. For $16 \leqslant z \leqslant 20$, the gas temperature in the preform tube is high enough for $GeCl_4$ oxidation to be at equilibrium (Fig. 1(a)). The K_{EQ} decreases as the gas temperature increases for $16 \leqslant z \leqslant 20$ and the $GeCl_4$ concentration increases, while the Cl_2 and GeO_2 concentrations decrease (Figs. 1(a)–(d) and (f)). For $z > 20$, the gas stream cools down by heat transfer to the preform tube wall. K_{EQ} increases, X_{GC} decreases and X_{CL} increases (Figs. 1(a), (b), (d) and (f)). Germania particles deposit to the tube wall by thermophoresis but at $z = 21$, the GeO_2 concentration near the tube wall increases by the fast forward reaction of $GeCl_4$ oxidation (there, K_{EQ} is higher than at $z = 20$) and Y_{GO} increases (Figs. 1(e) and (f)). Further downstream, the prevailing lower temperature slows down and effectively stops the $GeCl_4$ oxidation. Thus, the concentration profiles of $GeCl_4$ and Cl_2 become flattened by radial diffusion while the concentration of GeO_2 decreases by thermophoresis along the deposition zone of the preform tube.

In the MCVD process, the movement of particles

Table 1. Simulation conditions for the MCVD process with $SiCl_4$ and $GeCl_4$

$X_{SC,0}$	0–0.1
$X_{GC,0}$	0.043
$X_{O2,0}$	0.85–0.97
L_1 and L_2	20 and 22 cm
K	0.55
p_0	1 atm
Q	1–7 lpm
R	1 cm
T_0	800 °C
T_{max}	1700 °C
T_{min}	180 °C
E_{GC}	263 kJ mol^{-1}
E_{SC}	402 kJ mol^{-1}
$k_{GC,0}$	2.3×10^{15} cm^3 mol^{-1} s^{-1}
$k_{SC,0}$	1.7×10^{14} s^{-1}
$k_{SC,1}$	3.1×10^{19} cm^3 mol^{-1} s^{-1}
v_0	1.39×10^{-5}
ΔH_{GC}	46 kJ mol^{-1}
ΔH_{SC}	251 kJ mol^{-1}
$D_{GC,0}$, $D_{SC,0}$	6.0×10^{-6}, 6.32×10^{-6}
$D_{CL,0}$, $D_{O2,0}$	1.12×10^{-5}, 1.76×10^{-5}
C_{p0}, C_{p1}, C_{p2}	7.16, 1.0×10^{-3}, -0.4×10^{5}
k_0, k_1, k_2	1.08×10^{-5}, 1.82×10^{-7}, -2.34×10^{-11}

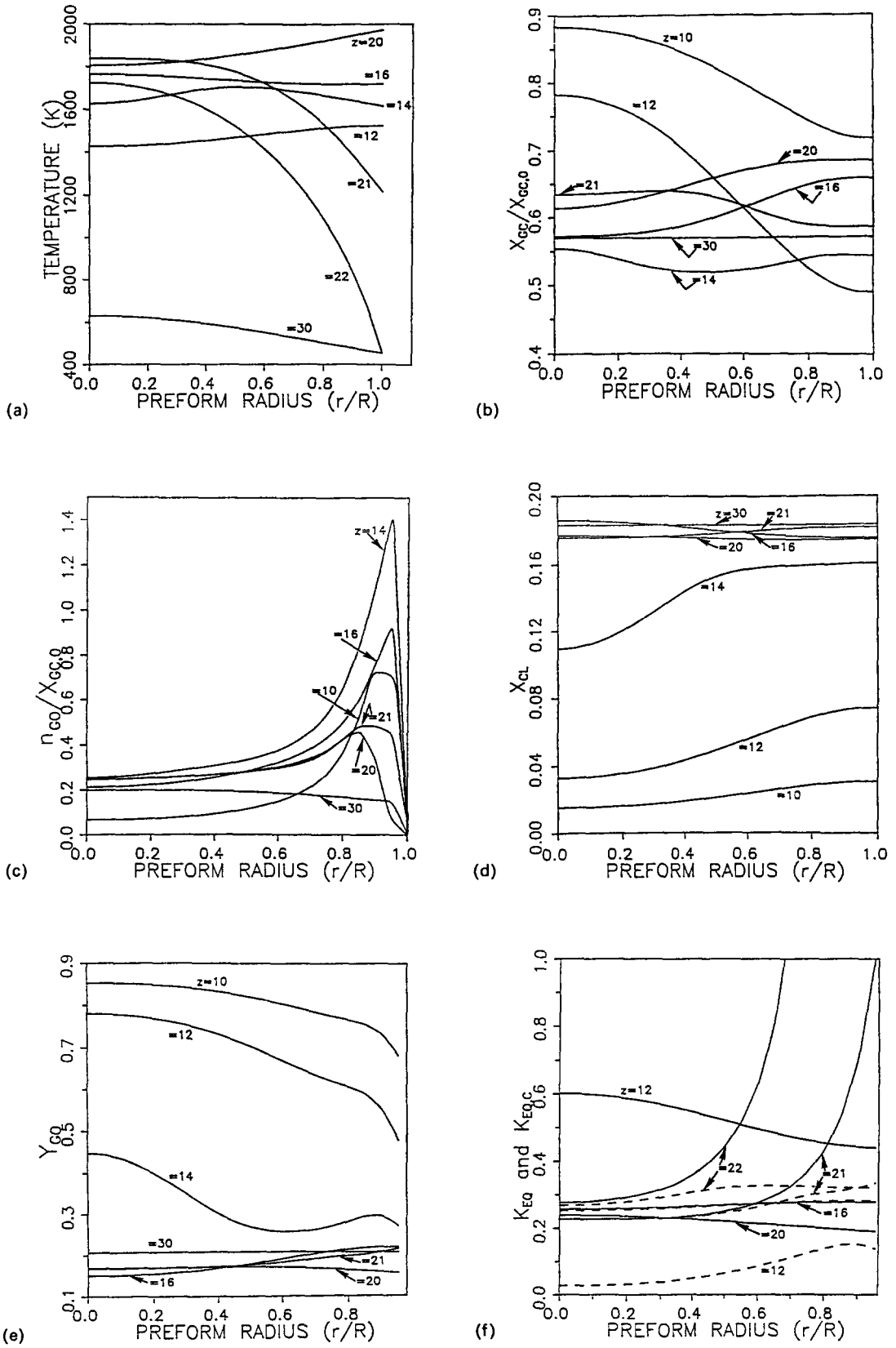

FIG. 1. Evolution of radial profiles of gas temperature (a), dimensionless $GeCl_4$ concentration (b), GeO_2 mass concentration (c), mole fraction of Cl_2 (d), mole fraction of GeO_2 in particle phase (e) and K_{EQ} (solid lines) and $K_{EQ,C}$ (dashed lines) (f) along the preform axis ($Q = 1$ lpm, $C_{SC,0} = 3 \times 10^{-6}$ mol cm^{-3} and $C_{GC,0} = 1.9 \times 10^{-6}$ mol cm^{-3}).

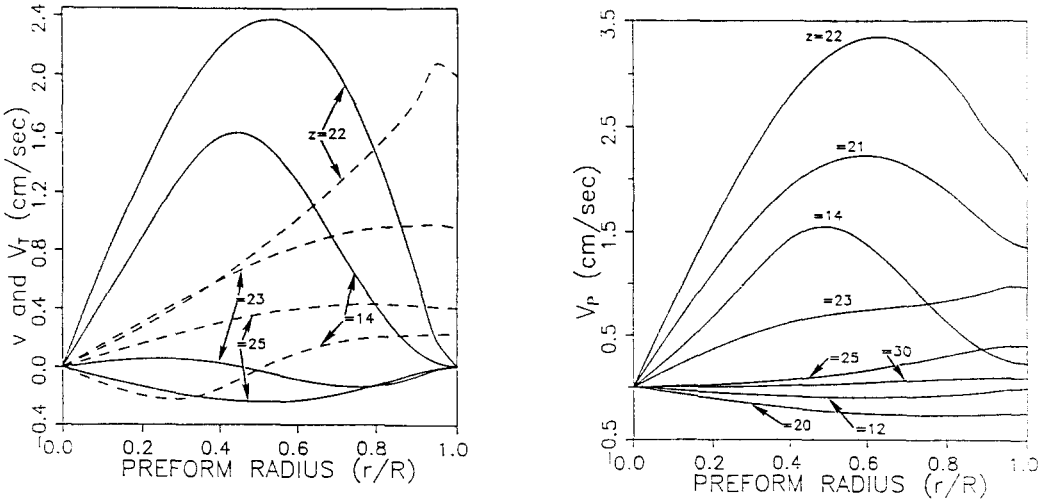

FIG. 2. Evolution of radial profiles of radial velocity of gas stream (solid lines) and thermophoretic velocity of particles (dashed lines) (a) and net particle velocity (V_P) (b) along the preform axis (Q = 1 lpm, $C_{SC,0} = 3 \times 10^{-6}$ mol cm^{-3} and $C_{GC,0} = 1.9 \times 10^{-6}$ mol cm^{-3}).

in the radial direction is important because it is closely related to overall process efficiency. The net particle velocity in the radial direction (V_P) is the sum of the radial gas velocity (v) and the radial thermophoretic velocity ($V_T = Kv\,\partial \ln T/\partial r$). The evolution of v and V_T and V_P is shown in Figs. 2(a) and (b) along the MCVD preform tube. The three velocities are all zero at the tube center. At the beginning of the preform tube ($z \leqslant 12$), v is negligible and V_T and V_P are negative; particles move toward the tube center by thermophoresis. At $z = 14$, the $SiCl_4$ oxidation is fast and v is significant around $r/R = 0.5$ because of the released heat of reaction and, therefore, particles move toward the tube wall. At $16 \leqslant z \leqslant 20$, the oxidation of $SiCl_4$ has been completed and V_P is toward the tube center again by thermophoresis. At $20 < z \leqslant 22$, v, V_T and V_P are fairly high and directed toward the tube wall. Further downstream ($z \geqslant 24$), the direction of v is toward the tube center, but those of V_T and V_P are still toward the tube wall. In the MCVD process, v is found to be important in pumping the particles located at $r/R = 0.5$ toward the tube wall when the $SiCl_4$ reaction is fast ($z = 14$) and the gas stream starts to cool down ($20 < z \leqslant 22$). From these results, the radial velocities are also expected to be important in analyzing the particle transport in aerosol flow reactors for fine particle production at high temperature [29, 30].

The predicted conversions and deposition efficiencies of $SiCl_4$ and $GeCl_4$ are shown along the preform axis in Fig. 3. The $SiCl_4$ conversion is complete and its deposition efficiency reaches 60%. The $GeCl_4$ conversion increases at the beginning of the reaction zone as the gas temperature increases. When the gas temperature is high enough ($T > 1680$ K) at the end of the reaction zone ($14 < z \leqslant 20$) (Fig. 1(a)), the $GeCl_4$ reaction is in equilibrium and the $GeCl_4$ conversion decreases along the preform axis. For $14 < z \leqslant 15$, the $GeCl_4$ conversion decreases rapidly as the gas temperature and Cl_2 concentration increase. After $z = 20$, the gas temperature starts to decrease and the $GeCl_4$ conversion increases again and reaches 43% and the overall deposition efficiency of GeO_2 is 26% at the employed process conditions. Rapid cooling of the gas stream in the deposition zone quenches the $GeCl_4$ oxidation and the $GeCl_4$ conversion and GeO_2 incorporation are determined by the equilibrium state of $GeCl_4$ oxidation at 1700 K, which is the gas temperature immediately downstream from the torch.

The effect of Soret diffusion of chemical species is also investigated in the present analysis for the process conditions of Fig. 1. The thermal diffusion factors of each chemical species are calculated using the

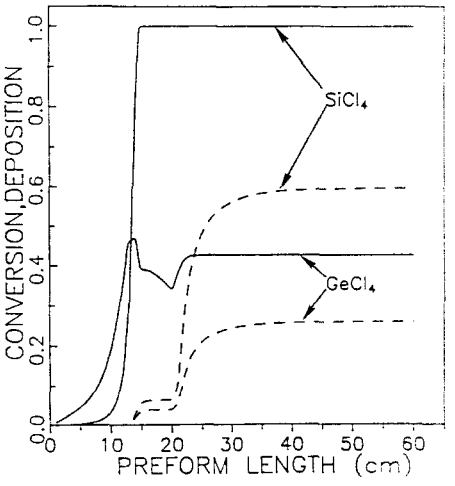

FIG. 3. $SiCl_4$ and $GeCl_4$ conversions (solid lines) and deposition efficiencies (dashed lines) along the preform axis, Q = 1 lpm, $C_{SC,0} = 3 \times 10^{-6}$ mol cm^{-3} and $C_{GC,0} = 1.9 \times 10^{-6}$ mol cm^{-3}.

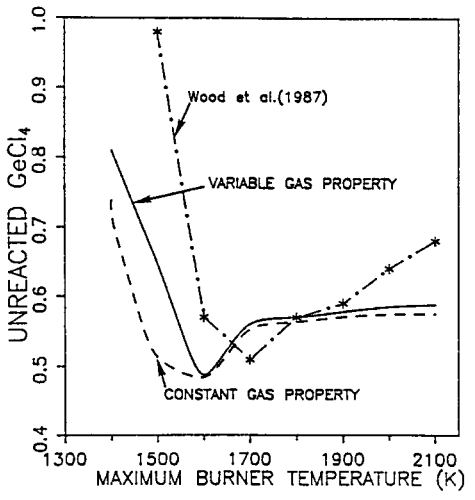

FIG. 4. Comparison of the model results with the experimental data by Wood *et al.* [2]. The results for 'variable gas property' (solid line) are from the present model and those of 'constant gas property' (dashed line) are from the model proposed by Kim and Pratsinis [11] ($Q = 1.72$ lpm, $C_{SC,0} = 3 \times 10^{-6}$ mol cm^{-3} and $C_{GC,0} = 1.9 \times 10^{-6}$ mol cm^{-3}).

expression by Rosner (see equation (2.3), Figs. 2 and 3 of ref. [31]). The effect of Soret diffusion is negligible for $0 \leqslant z \leqslant 20$ because of the low temperature gradient (Fig. 1(a)). The $SiCl_4$ conversion is complete before $z = 20$ (Fig. 3) and the $SiCl_4$ yield is not affected by Soret diffusion. Because of the steep temperature gradient for $21 \leqslant z \leqslant 25$, the $GeCl_4$ and Cl_2 concentrations with Soret diffusion are a little higher near the tube wall and lower at the tube center than the results of Figs. 1(b) and (d), but the overall $GeCl_4$ conversion and deposition efficiency with Soret diffusion are close to the results of Fig. 3.

The present results for $GeCl_4$ conversion are compared with the experimental results of Wood *et al.* [2] in Fig. 4. The results for 'constant gas properties' are from the model proposed by Kim and Pratsinis [11] when gas properties at the average process temperature are employed. The results for 'variable gas properties' are from the present model. For low T_{max} ($T_{max} \leqslant 1600$ K), the forward reaction rate of $GeCl_4$ oxidation increases as T_{max} increases, but the gas temperature is not high enough to reach the equilibrium state of $GeCl_4$ oxidation. So the unconverted $GeCl_4$ decreases as T_{max} increases. At $T_{max} = 1600$ K, the gas temperature is high enough for $GeCl_4$ oxidation but not high enough for $SiCl_4$ oxidation. As the Cl_2 concentration is not high by incomplete $SiCl_4$ conversion, the $GeCl_4$ conversion reaches a maximum at $T_{max} = 1600$ K. At higher T_{max} ($\geqslant 1700$ K), the outlet Cl_2 concentration increases since the $SiCl_4$ is fully oxidized and the K_{EQ} for the $GeCl_4$ oxidation decreases with temperature and subsequently, the unreacted $GeCl_4$ increases. Overall, the model results with variable gas properties are in better agreement with the experimental data than the model results with constant gas properties. The numerical results also show that the $GeCl_4$ conversion reaches a maximum at $T_{max} = 1600$ K when another ratio of inlet $GeCl_4$ and $SiCl_4$ concentrations is applied ($C_{GC,0} = 1 \times 10^{-6}$ mol cm^{-3}, $C_{SC,0} = 3 \times 10^{-6}$ mol cm^{-3}).

There is, however, some disagreement between the numerical results and the experimental data in Fig. 4. Specifically, the numerical calculations underpredict the $GeCl_4$ conversion at low ($T_{max} < 1600$ K) and high ($T_{max} > 1800$ K) temperatures. For all numerical simulations, the same T_0 ($= 1073$ K) is used at all T_{max}. In actual MCVD processes, however, T_0 will decrease as T_{max} decreases. If a lower T_0 is applied with low T_{max} in the numerical simulation, the unconverted $GeCl_4$ will increase and better agreement with the experimental data is obtained.

At high T_{max} (> 1800 K), the experimentally measured, unconverted $GeCl_4$ concentration is higher than that calculated by the present model (Fig. 4). The $GeCl_4$ conversion is low just above the torch since the $GeCl_4$ reaction equilibrium is unfavorable at high temperature. After the torch, the $GeCl_4$ conversion increases again as the gas temperature decreases, and new GeO_2 particles are produced. The newly formed GeO_2 particles coagulate and deposit onto the existing GeO_2/SiO_2 particles, creating higher GeO_2 concentration at the particle surface than its center. In the numerical simulations, it is assumed that Y_{GO} is uniform throughout the particle. In reality, Y_{GO} near the particle surface will be higher than at the particle center. This increases the rate of the reverse reaction of $GeCl_4$ oxidation and the amount of unconverted $GeCl_4$ in the deposition zone becomes higher than the predictions of the numerical simulation. The higher the torch temperature is, the lower the $GeCl_4$ conversion is just above the torch, forming more of a shell of GeO_2 near the particle surface and making the unconverted $GeCl_4$ concentration higher in the effluents. The formation of a shell rich in GeO_2 at the surface of GeO_2/SiO_2 soot particles has also been reported in experimental studies of vapor-phase axial deposition processes [32].

In Fig. 5, the $GeCl_4$ conversion and deposition efficiency are shown for various inlet $SiCl_4$ concentrations as a function of total gas flow rate. As inlet $SiCl_4$ concentration increases, the $GeCl_4$ conversion and deposition efficiency decrease since more Cl_2 is produced by the $SiCl_4$ oxidation. Thus, the $GeCl_4$ reaction is shifted to the left. The $GeCl_4$ conversion and deposition efficiency in the absence of $SiCl_4$ ($C_{SC,0} = 0$) are 70 and 44%, respectively, while, with $C_{SC,0} = 5 \times 10^{-6}$ mol cm^{-3}, they are 33.5 and 21%. At low inlet $SiCl_4$ concentration and high overall gas flow rate, the MCVD process is limited by the rate of $GeCl_4$ oxidation and, therefore, $GeCl_4$ conversion and deposition efficiency decrease as total gas flow rate increases (this is equivalent to reducing the process residence time). At high inlet $SiCl_4$ concentration, the gas temperature increases significantly as a result of the released heat of $SiCl_4$ reaction; the

cal kinetics of $SiCl_4$, $SiBr_4$, $GeCl_4$, $POCl_3$, and BCl_3 with oxygen, *J. Phys. Chem.* **82**, 2191–2194 (1978).
17. D. E. Rosner and H. M. Park, Thermophoretically augmented mass-, momentum- and energy-transfer rates in high particle mass loaded laminar forced convection systems, *Chem. Engng Sci.* **43**, 2689–2704 (1988).
18. H. M. Park and D. E. Rosner, Multiphase continuum theory of dopant redistribution across aerosol-laden laminar nonisothermal boundary layers, *Chem. Engng Sci.* **44**, 603–617 (1989).
19. R. C. Reid, J. M. Prausnitz and T. K. Sherwood, *The Properties of Gases and Liquids* (3rd Edn). McGraw-Hill, New York (1977).
20. J. M. Smith and H. C. Van Ness, *Introduction to Chemical Engineering Thermodynamics* (3rd Edn). McGraw-Hill, New York (1975).
21. R. H. Perry and D. Green, *Perry's Chemical Engineers' Handbook* (6th Edn). McGraw-Hill, New York (1984).
22. J. H. Ferziger, *Numerical Methods for Engineering Applications*. Wiley, New York (1981).
23. IMSL, *IMSL Contents Document* (8th Edn). International Mathematical and Statistical Libraries, Houston (1980).
24. C. F. Gerald and P. O. Wheatley, *Applied Numerical Analysis* (3rd Edn). Addison-Wesley, Reading, Massachusetts (1984).
25. D. A. Anderson, J. C. Tannerhill and R. H. Pletcher, *Computational Fluid Mechanics and Heat Transfer*. McGraw-Hill, New York (1984).
26. K.-S. Kim, Fabrication of optical fiber preforms by modified chemical vapor deposition, Ph.D. Thesis, University of Cincinnati, Ohio (1989).
27. P. M. Worsoe-Schmidt and G. Leppert, Heat transfer and friction for laminar flow of gas in a circular tube at high heating rate, *Int. J. Heat Mass Transfer* **8**, 1281–1301 (1965).
28. R. B. Bird, W. E. Stewart and E. N. Lightfoot, *Transport Phenomena*. Wiley, New York (1960).
29. K. Okuyama, Y. Kousaka, N. Tohge, S. Yamamoto, J. J. Wu, R. C. Flagan and J. H. Seinfeld, Production of ultrafine metal oxide aerosol particles by thermal decomposition of metal alkoxide vapors, *A.I.Ch.E. Jl* **32**, 2010–2019 (1986).
30. J. J. Wu and R. C. Flagan, Onset of runaway nucleation in aerosol reactors, *J. Appl. Phys.* **61**, 1365–1371 (1987).
31. D. E. Rosner, Thermal (Soret) diffusion effects on interfacial mass transport rates, *J. PhysicoChem. Hydrodynam.* **1**, 159–185 (1980).
32. D. L. Wood, E. Potkay, H. R. Clark and T. Y. Kometani, Characterization of torch-deposited silica for light-guide preforms, *Appl. Spectr.* **42**, 299–304 (1988).

DEPOT SIMULTANE DE SiO_2/GeO_2 PENDANT LA PRODUCTION DE PREFORMES DE FIBRES OPTIQUES PAR DEPOSITION CHIMIQUE DE VAPEUR MODIFIEE

Résumé—On présente une étude théorique de transferts simultanés de chaleur et de masse pendant le mécanisme de dépôt chimique modifié multicomposant de vapeur (MCVD) pour la fabrication de préformes de guide de lumière. Le dépôt simultané de SiO_2 et GeO_2 est examiné car ce sont les espèces dominantes des guides de lumière pour les télécommunications. Les équations complètes de Navier–Stokes sont résolues en incluant les bilans de quantité de mouvement et d'énergie pour les gaz et les particules de SiO_2 et GeO_2. La conversion de $GeCl_4$ et l'efficacité du dépôt diminuent quand la concentration de $SiCl_4$ augmente. Aux débits élevés de gaz à travers le tube de préforme et pour de faibles concentrations de $SiCl_4$ à l'entrée, la production de $GeCl_4$ est limitée par la conversion de $GeCl_4$, tandis qu'aux faibles débits de gaz ou pour des concentrations élevées de $SiCl_4$ à l'entrée, la production de $GeCl_4$ est limitée par le transport des particules.

DIE GLEICHZEITIGE ABLAGERUNG VON SiO_2 UND GeO_2 BEI DER HERSTELLUNG OPTISCHER FASER-HALBZEUGE DURCH MODIFIZIERTE CHEMISCHE DAMPFABSCHEIDUNG

Zusammenfassung—Es wird eine theoretische Studie über die gekoppelten Vorgänge beim Wärme- und Stofftransport mit chemischer Reaktion beim sogenannten modifizierten chemischen Mehrkomponenten-Dampfabscheideverfahren (MCVD) zur Herstellung von Lichtleiter-Halbzeugen vorgestellt. Die gleichzeitige Ablagerung von SiO_2 und GeO_2 wird untersucht, da dies die wichtigsten Stoffe für Lichtleiter im Telekommunikationsbereich sind. Die vollständigen Navier–Stokes-Gleichungen werden aufgrund der Stoff-, Impuls-, Energie- und Massen-Bilanzen für die Gase und die SiO_2- und GeO_2-Partikel formuliert und gelöst. Der Grad der $GeCl_4$-Umwandlung und -ablagerung nimmt mit steigender $SiCl_4$-Konzentration am Eintritt ab. Bei hohen Gasströmungsgeschwindigkeiten und geringer $SiCl_4$-Konzentration am Eintritt wird die $GeCl_4$-Ausbeute durch die $GeCl_4$-Umwandlung begrenzt. Hingegen ist bei geringen Gasgeschwindigkeiten und hoher $SiCl_4$-Konzentration am Eintritt die $GeCl_4$-Ausbeute durch den Partikeltransport begrenzt.

СОВМЕСТНОЕ ОСАЖДЕНИЕ SiO_2 И GeO_2 В ПРОЦЕССЕ ПРОИЗВОДСТВА БРИКЕТОВ ИЗ ОПТИЧЕСКОГО ВОЛОКНА МЕТОДОМ МОДИФИЦИРОВАННОГО ХИМИЧЕСКОГО ОСАЖДЕНИЯ ПАРА

Аннотация—Теоретически исследуется сложный тепло- и массоперенос при химической реакции в процессе так называемого модифицированного химического осаждения многокомпонентного пара при изготовлении световодных брикетов. Рассматривается совместное осаждение SiO_2 и GeO_2, т. к. они составляют основу световодов, используемых для телекоммуникаций. Решаются полные уравнения Навье–Стокса, включающие балансы неразрыности, импульса энергии и массы для газов и частиц SiO_2 и GeO_2. Эффективность конвекции и осаждения $GeCl_4$ снижается с ростом концентрации $SiCl_4$ на входе. При высоких суммарных расходах газа выход $GeCl_4$ ограничен его конверсией, в то время как при низких расходах газа или высоких концентрациях $SiCl_4$ на входе выход $GeCl_4$ ограничен переносом частиц.

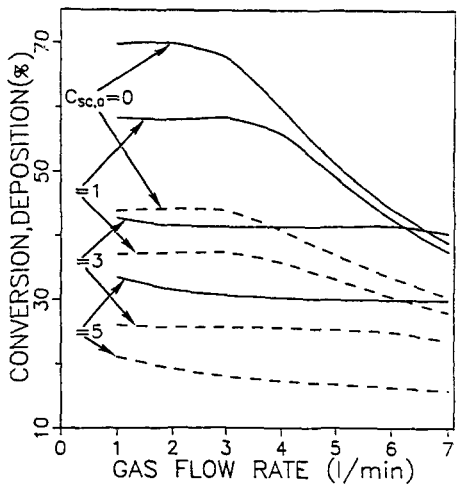

FIG. 5. $GeCl_4$ conversions (solid lines) and GeO_2 deposition efficiencies (dashed lines) as a function of overall carrier gas flow rate at various inlet $SiCl_4$ concentrations and constant inlet $GeCl_4$ concentration ($C_{GC,0} = 1.9 \times 10^{-6}$ mol cm^{-3}). The units of $C_{SC,0}$ are in 10^{-6} mol cm^{-3}.

$GeCl_4$ reaction is in equilibrium even at high gas flow rates and the $GeCl_4$ conversion and deposition efficiency maintain almost constant values for all gas flow rates.

As the $GeCl_4$ conversion is higher in the absence of $SiCl_4$, the $GeCl_4$ yield can be improved by alternatively supplying $GeCl_4$ and $SiCl_4$ vapors to the preform tube, making, thus, ultrathin layers of pure GeO_2 and SiO_2. As the GeO_2 is redistributed between each layer during fusion of the particle deposits by the heat from the moving torch, the attainment of a smooth radial refractive index profile in the optical fiber can be achieved. In this case, the refractive index profile can be adjusted by controlling the thicknesses of each GeO_2 and SiO_2 layer.

CONCLUSIONS

Manufacture of graded index optical fiber preforms by multicomponent modified chemical vapor deposition of SiO_2 and GeO_2 is theoretically investigated. The Navier–Stokes equations for this process are developed and numerically solved.

The radial and thermophoretic velocities are important for the particle transport in the MCVD process. At low temperature ($T \leqslant 1700$ K), the forward reaction of $GeCl_4$ oxidation is found to be faster than the backward reaction both in the beginning of the reaction zone and in the deposition zone. At high temperature ($T \geqslant 1700$ K), the $GeCl_4$ oxidation is in equilibrium at the end of the reaction zone. The $GeCl_4$ conversion and GeO_2 incorporation in MCVD are found to be controlled by the equilibrium constant of $GeCl_4$ oxidation at $T = 1700$ K. The predicted model results for the $GeCl_4$ conversion are shown to be in good agreement with experimental data. The $GeCl_4$ conversion and deposition efficiency decrease as inlet $SiCl_4$ concentration increases and also decrease as the total gas flow rate increases at low inlet $SiCl_4$ concentrations because the $GeCl_4$ conversion is incomplete. The proposed model can be applied to predict the incorporation of GeO_2 in lightguide preforms by oxidation of $SiCl_4$ and $GeCl_4$ for accurate control of the refractive index profile of optical fibers.

Acknowledgements—This work was partially supported by the Center for Aerosol Processes which was established by the Ohio Board of Regents through the Research Challenge Program and by the National Science Foundation, Grant CBT-8707144. The authors acknowledge helpful discussions with Dr P. Biswas of the University of Cincinnati and constructive comments by Dr D. E. Rosner from Yale University.

REFERENCES

1. S. R. Nagel, J. B. MacChesney and K. L. Walker, An overview of the modified chemical vapor deposition (MCVD) process and performance, *IEEE J. Quantum Electron.* **QE-18,** 459–476 (1982).
2. D. L. Wood, K. L. Walker, J. B. MacChesney, J. R. Simpson and R. Csencsits, Germanium chemistry in the MCVD process for optical fiber fabrication, *J. Lightwave Technol.* **LT-5,** 277–285 (1987).
3. J. B. MacChesney, P. B. O'Connor and H. M. Presby, A new technique for preparation of low-loss and graded index optical fibers, *Proc. IEEE* **62,** 1280–1281 (1974).
4. P. G. Simpkins, S. Greenberg-Kosinski and J. B. MacChesney, Thermophoresis: the mass transfer mechanism in modified chemical vapor deposition, *J. Appl. Phys.* **50,** 5676–5681 (1979).
5. K. L. Walker, F. T. Geyling and S. R. Nagel, Thermophoretic deposition of small particles in the modified chemical deposition (MCVD) process, *J. Am. Ceram. Soc.* **63,** 552–558 (1980).
6. T. F. Morse and J. W. Cipolla, Jr., Laser modification of thermophoretic deposition, *J. Colloid Interface Sci.* **97,** 137–148 (1984).
7. T. F. Morse, C. Y. Wang and J. W. Cipolla, Jr., Laser-induced thermophoresis and particulate deposition efficiency, *ASME J. Heat Transfer* **107,** 155–160 (1985).
8. T. F. Morse, D. DiGiovanni, C. Y. Wang and J. W. Cipolla, Jr., Laser enhancement of thermophoretic deposition processes, *J. Lightwave Technol.* **4,** 151–155 (1986).
9. M. Fiebig, M. Hilgenstock and A.-A. Riemann, The modified chemical vapor deposition process in a concentric annulus, *Aerosol Sci. Technol.* **9,** 237–249 (1988).
10. S. E. Pratsinis and K.-S. Kim, Particle coagulation, diffusion and thermophoresis in laminar tube flows, *J. Aerosol Sci.* **20,** 101–111 (1989).
11. K.-S. Kim and S. E. Pratsinis, Manufacture of optical waveguide preforms by modified chemical vapor deposition, *A.I.Ch.E. Jl* **34,** 912–921 (1988).
12. K.-S. Kim and S. E. Pratsinis, Modeling and analysis of modified chemical vapor deposition of optical fiber preforms, *Chem. Engng Sci.* **44,** 2475–2482 (1989).
13. M. P. Bohrer, J. A. Amelse, P. L. Narasimham, B. K. Tariyal, J. M. Turnipseed, R. F. Gill, W. J. Moebuis and J. L. Bodeker, A process for recovering germanium from effluents of optical fiber manufacturing, *J. Lightwave Technol.* **LT-3,** 699–705 (1985).
14. W. M. Kays and H. C. Perkins, *Handbook of Heat Transfer* (Edited by W. M. Rohsenow, J. P. Hartnett and E. N. Ganic) (2nd Edn), Chap. 7. McGraw-Hill, New York (1985).
15. D. R. Powers, Kinetics of $SiCl_4$ oxidation, *J. Am. Ceram. Soc.* **61,** 295–297 (1978).
16. W. G. French, L. J. Pace and V. A. Foertmeyer, Chemi-